Direct reconstruction of p-p elastic scattering amplitudes at 1.8 and 2.1 GeV

Nader Ghahramany and Ghasem Forozani
Department of Physics, Shiraz University, Shiraz 71454, Iran
(Received 22 June 1999; revised manuscript received 16 December 1999; published 8 May 2000)

The direct reconstruction of the proton-proton elastic-scattering complex amplitudes is carried out at 1.8 and 2.1 GeV. Five independent amplitudes both in helicity and transversity frame were obtained by using an extensive set of data measured recently at SATURNE II and by the EDDA (COSY) Collaboration. The real and imaginary parts of the amplitudes are plotted versus different interpolated c.m. angles for both frames. Four distinct sets of solutions exist, one of which is chosen on the basis of minimum χ^2.

PACS number(s): 13.75.Cs, 13.85.−t

I. INTRODUCTION

In spite of the fact that more than three decades have passed since the first amplitude analysis was performed in elastic p-p scattering, a direct reconstruction of amplitudes still seems to be quite attractive for the following reasons: first, the dynamical models have not yet been able to give us a clear picture of nucleon-nucleon scattering which is the basic reaction necessary to understand the nature of nuclear forces. Second, the spin effects of the nucleon constituents can be investigated in detail by using new polarized beams and polarized targets and measuring new polarization parameters from which amplitudes are nondynamically obtained. Third, several accelerators have been able to produce polarized beams of protons and neutrons over a wide range of energies. Also new target materials have been developed providing better target polarization via the frozen-spin mode [1].

In the energy range of below 1 GeV for p-p elastic scattering, partial wave analysis has successfully provided unambiguous phase shifts as a function of energy [2]. At higher energies such partial wave analysis is complicated [3] and instead, it is better to obtain the reaction amplitudes by direct reconstruction using the optimal formalism of polarization analysis [4]. Using such optimal formalism five complete reaction amplitudes were determined at 6 GeV by one of us (N.Gh) using polarization data obtained at the Argonne Zero Gradient Synchrotron (AZGS) for elastic p-p scattering in 1982 [5]. On the basis of such analysis, the Regge pole as well as particle exchange models have been tested [6].

Since the shut down of AZGS, this is the first time that an almost complete set of observables is measured at SATURNE II.

A complete set of experiments as defined in Ref. [7] is an example of observables to be measured, if it contains sufficient information for an exhaustive description of the interaction, i.e., for a complete determination of the complex amplitudes. It has been established [8] that ten appropriately chosen observables including the differential cross section could form a complete set in p-p elastic scattering from which a direct reconstruction of the scattering matrix element can be performed by imposition of only symmetry properties [9].

The imposition of symmetry constraints [10] not only constrains the choices of the direction of the quantization axis, it also reduces the number of independent amplitudes from 16 to only 5.

The purpose of the present article is to report such a complete amplitude reconstruction for p-p elastic scattering at 1.8 and 2.1 GeV for the entire range of 65° to 101° c.m. angles measured most recently at SATURNE II in both transversity and helicity frames.

II. REACTION MATRIX AND OBSERVABLES

The general formalism in which our reaction matrix and observables are defined has been developed by Moravcsik in conjunction with two main collaborators, Csonka and Scadron in an extensive series of papers [11]. In particular the nondynamical structure of the reaction involving four spin-1/2 particles is carried out in Ref. [12]. The first amplitude analysis involving numerical calculations of five independent amplitudes in such formalism was performed due to availability of data from AZGS [5]. We do not intend to go into the details of the structure and polarization analysis of the reaction matrix, instead we attempt to perform a complete determination of the amplitudes after a brief introduction of the reaction matrix and observables in order to obtain a general relationship between the observables and bilinear combination of amplitudes in the p-p reaction. The standard factorization procedure is used [13] by decomposing the reaction into two constituent reactions, namely target recoil $(0+1/2\rightarrow 0+1/2)$ and beam scattered $(1/2+0\rightarrow 1/2+0)$. The outer product of the two constituent reaction matrices result in a composite reaction matrix.

Let us write the reaction matrix of the first constituent reaction by $M1$ where [11]

$$M1 = a_0 I + a_1 \boldsymbol{\sigma}\cdot\mathbf{l} + a_2 \boldsymbol{\sigma}\cdot\mathbf{m} + a_3 \boldsymbol{\sigma}\cdot\mathbf{n}, \tag{1}$$

where σ is Pauli vector matrix for spin 1/2 and I is identity matrix. Unit vectors $\mathbf{l}$, $\mathbf{m}$, and $\mathbf{n}$ are defined as

$$\mathbf{l} = \frac{\mathbf{q_C} - \mathbf{q_A}}{|\mathbf{q_C} - \mathbf{q_A}|}, \quad \mathbf{m} = \frac{\mathbf{q_A} \times \mathbf{q_C}}{|\mathbf{q_A} \times \mathbf{q_C}|}, \quad \mathbf{n} = \mathbf{l} \times \mathbf{m}, \tag{2}$$

where $\mathbf{q_i}$ are the center-of-mass momenta for the general reaction

$$A+B\rightarrow C+D. \tag{3}$$

Assuming similar results hold for the second constituent reaction and only rotational invariance, the reaction matrix for the composite reaction is

$$\begin{aligned} M = {} & D_0 + D_{10}(\boldsymbol{\sigma_1}\cdot\mathbf{l}) + D_{20}(\boldsymbol{\sigma_1}\cdot\mathbf{m}) + D_{30}(\boldsymbol{\sigma_1}\cdot\mathbf{n}) + D_{01}(\boldsymbol{\sigma_2}\cdot\mathbf{l}) \\ & + D_{02}(\boldsymbol{\sigma_2}\cdot\mathbf{m}) + D_{03}(\boldsymbol{\sigma_2}\cdot\mathbf{n}) + D_{11}(\boldsymbol{\sigma_1}\cdot\mathbf{l})(\boldsymbol{\sigma_2}\cdot\mathbf{l}) \\ & + D_{12}(\boldsymbol{\sigma_1}\cdot\mathbf{l})(\boldsymbol{\sigma_2}\cdot\mathbf{m}) + D_{13}(\boldsymbol{\sigma_1}\cdot\mathbf{l})(\boldsymbol{\sigma_2}\cdot\mathbf{n}) \\ & + D_{21}(\boldsymbol{\sigma_1}\cdot\mathbf{m})(\boldsymbol{\sigma_2}\cdot\mathbf{l}) + D_{22}(\boldsymbol{\sigma_1}\cdot\mathbf{m})(\boldsymbol{\sigma_2}\cdot\mathbf{m}) \\ & + D_{23}(\boldsymbol{\sigma_1}\cdot\mathbf{m})(\boldsymbol{\sigma_2}\cdot\mathbf{n}) + D_{31}(\boldsymbol{\sigma_1}\cdot\mathbf{n})(\boldsymbol{\sigma_2}\cdot\mathbf{l}) \\ & + D_{32}(\boldsymbol{\sigma_1}\cdot\mathbf{n})(\boldsymbol{\sigma_2}\cdot\mathbf{m}) + D_{33}(\boldsymbol{\sigma_1}\cdot\mathbf{n})(\boldsymbol{\sigma_2}\cdot\mathbf{n}), \end{aligned} \tag{4}$$

where $\boldsymbol{\sigma_1}$ and $\boldsymbol{\sigma_2}$ are Pauli matrices for projectile and target particles. The dynamics of the reaction is wholly contained within the invariant amplitudes D's in Eq. (4). The number of amplitudes in Eq. (4) is 16. In a more compact notation the first constituent reaction is denoted as

$$M1 = \sum_l \sum_\lambda D(\lambda,l) S^{\lambda l}, \tag{5}$$

where l and λ denote the spin component of target and recoil particles along the quantization axis. $D(\lambda,l)$ are amplitudes and $S^{\lambda l}$ are the spin-momentum tensors generally, but here they are a set of 2×2 matrices specified by the spin of each particle. The reaction is characterized by the initial and final density matrices ρ_i and ρ_f both being 2×2 matrices which describe the initial and final polarization states, respectively. In terms of the elements we have

$$\rho_i = \rho_i^{uv}, \quad u,v = 1,2, \tag{6}$$

the final density matrix is

$$\rho_f^{uv} = M \rho_i^{uv} M^\dagger, \tag{7}$$

and substituting for M from Eq. (5) we get

$$\rho_f^{uv} = \sum_l \sum_\lambda \sum_{l'} \sum_{\lambda'} D(\lambda,l) D^*(\lambda',l') S^{\lambda l} \rho_i^{uv} (S^{\lambda' l'})^\dagger. \tag{8}$$

Experimental observables are given by the expectation values of certain spin-momentum tensors F in the final states (exit channel). In matrix element notation we denote them by

$$F = F^{\xi\omega}, \quad \xi,\omega = 1,2. \tag{9}$$

Also we denote the experimental observables by L, then

$$\begin{aligned} L(uv;\xi\omega) &= \langle F^{\xi\omega} \rangle \\ &= \mathrm{Tr}(F^{\xi\omega} \rho_f^{\mu\nu}) \\ &= \mathrm{Tr}(F^{\xi\omega} M \rho_i^{\mu\nu} M^\dagger), \end{aligned} \tag{10}$$

substitute Eqs. (5) and (7) into Eq. (10) to get

TABLE I. Data set of observables used in the present analysis and their corresponding notations and the number of data points and their references, as well as the χ^2 per number of data, are summarized.

Observables			1.80 GeV		2.10 GeV	
Argonne	Bystricky	ARNDT	Ref.	Points	Ref.	Points
$\sigma = d\sigma/d\Omega$	I_{000}	$d\sigma/d\Omega$	15	20	[15]	14
P	$A_{00n0} = A_{000n}$	P	[24]	19	[21]	8
CNN	A_{00nn}	AYY	[17]	18	[18]	22
DNN	D_{0n0n}	D	[22,16]	6	[22,16]	6
KNN	K_{0nn0}	DT	[22,16]	6	[22,16]	6
CSL	A_{00sk}	AZX	[16]	20	[16]	20
CLL	A_{00kk}	AZZ	[19]	19	[19]	18
CSS	A_{00ss}	AXX	[20]	20	[20]	14
KSS	$K_{0s''s0}$	RT	[16]	3	[16]	3
$HSNS$	$N_{0s''s0}$	NSSN	[16]	3	[16]	3
	Total points			134		114
	χ^2/data		1.07		0.83	

TABLE II. Results of the magnitudes of transversity amplitudes at 1.8 GeV.

$\theta_{\text{c.m.}}$	$\lvert\alpha\rvert$	$\lvert\beta\rvert$	$\lvert\gamma\rvert$	$\lvert\delta\rvert$	$\lvert\varepsilon\rvert$
65	0.335±0.011	0.309±0.012	0.247±0.015	0.090±0.041	0.068±0.055
67	0.352±0.011	0.314±0.012	0.238±0.016	0.095±0.040	0.091±0.041
69	0.345±0.013	0.313±0.015	0.211±0.022	0.099±0.047	0.121±0.038
71	0.336±0.014	0.308±0.015	0.183±0.026	0.102±0.046	0.139±0.034
73	0.320±0.012	0.283±0.013	0.153±0.025	0.098±0.038	0.143±0.026
75	0.328±0.012	0.285±0.014	0.142±0.027	0.099±0.039	0.155±0.025
77	0.305±0.011	0.287±0.011	0.129±0.025	0.096±0.034	0.151±0.022
79	0.310±0.011	0.291±0.011	0.130±0.025	0.100±0.033	0.144±0.023
81	0.313±0.010	0.296 ±0.011	0.142±0.022	0.099±0.032	0.134±0.024
83	0.301±0.010	0.289±0.010	0.148±0.020	0.093±0.032	0.116±0.025
85	0.324±0.011	0.326±0.011	0.169±0.021	0.101±0.035	0.115±0.031
87	0.299±0.010	0.297±0.010	0.146±0.021	0.095±0.032	0.100±0.030
89	0.297±0.011	0.308±0.010	0.137±0.023	0.100±0.032	0.114±0.028
90	0.299±0.011	0.308±0.010	0.129±0.025	0.098±0.032	0.127±0.025
91	0.298±0.011	0.305±0.011	0.118±0.027	0.098±0.033	0.137±0.023
93	0.290±0.011	0.303±0.011	0.096±0.034	0.098±0.034	0.148±0.022
95	0.318±0.013	0.333±0.012	0.106±0.037	0.103±0.039	0.173±0.023
97	0.288±0.012	0.302 ±0.011	0.105 ±0.031	0.093±0.036	0.156±0.021
99	0.296±0.013	0.313±0.012	0.123±0.027	0.098±0.034	0.151±0.022
101	0.291±0.013	0.310±0.012	0.139±0.023	0.099±0.033	0.135±0.024

$$L(uv;\xi\omega)=\sum_{l}\sum_{\lambda}\sum_{l'}\sum_{\lambda'}D(\lambda,l)D^{*}(\lambda',l')\times\sum_{\alpha}\sum_{\beta}\sum_{a}\sum_{b}(F^{\xi\omega})_{\beta\alpha}(S^{\lambda l})_{\alpha a}\times(\rho_{i}^{uv})_{ab}(S^{\lambda' l'})_{b\beta}. \tag{11}$$

Optimal formalism is a particular representation in which spin-momentum matrix, initial and final density matrices are defined in a way such that the elements of the observable-bilinear combination of amplitudes matrix is as diagonal as possible. Therefore, ρ_i, ρ_f, and observables F all have to be chosen to be Hermitian. For the composite reaction the reaction matrix is written

$$M=\sum_{\lambda}\sum_{l}\sum_{\Lambda}\sum_{L}D(\lambda l,\Lambda L)S^{\lambda l}\otimes S^{\Lambda L}, \tag{12}$$

where $S^{\lambda l}$ and $S^{\Lambda L}$ denote 2×2 spin momentum matrices for the beam-scattered and target-recoil particles, respectively.

TABLE III. Results of the magnitudes of transversity amplitudes at 2.1 GeV.

$\theta_{\text{c.m.}}$	$\lvert\alpha\rvert$	$\lvert\beta\rvert$	$\lvert\gamma\rvert$	$\lvert\delta\rvert$	$\lvert\varepsilon\rvert$
69	0.296±0.009	0.217±0.012	0.186±0.014	0.125±0.020	0.055±0.046
71	0.292±0.009	0.223±0.012	0.174±0.015	0.110±0.024	0.064±0.041
73	0.295±0.010	0.232±0.012	0.168±0.016	0.094±0.029	0.078±0.035
75	0.282±0.011	0.226±0.013	0.162±0.019	0.076±0.039	0.085±0.035
77	0.269±0.011	0.220±0.013	0.158±0.018	0.077±0.038	0.076±0.038
79	0.258±0.011	0.217±0.013	0.150±0.019	0.092±0.031	0.063±0.045
83	0.230±0.010	0.205±0.011	0.124±0.018	0.107±0.021	0.078±0.029
85	0.251±0.012	0.232±0.013	0.124±0.024	0.124±0.024	0.105±0.028
87	0.236±0.009	0.228±0.009	0.104±0.020	0.118±0.018	0.117±0.018
89	0.258±0.010	0.256±0.010	0.094±0.026	0.122±0.020	0.139±0.017
91	0.263±0.011	0.265±0.011	0.085±0.032	0.098±0.028	0.149±0.018
95	0.235±0.009	0.252±0.009	0.100±0.021	0.128±0.016	0.120±0.017
97	0.197±0.009	0.223±0.008	0.096±0.018	0.112±0.016	0.119±0.015
99	0.226±0.011	0.264±0.010	0.073±0.034	0.109±0.023	0.149±0.017

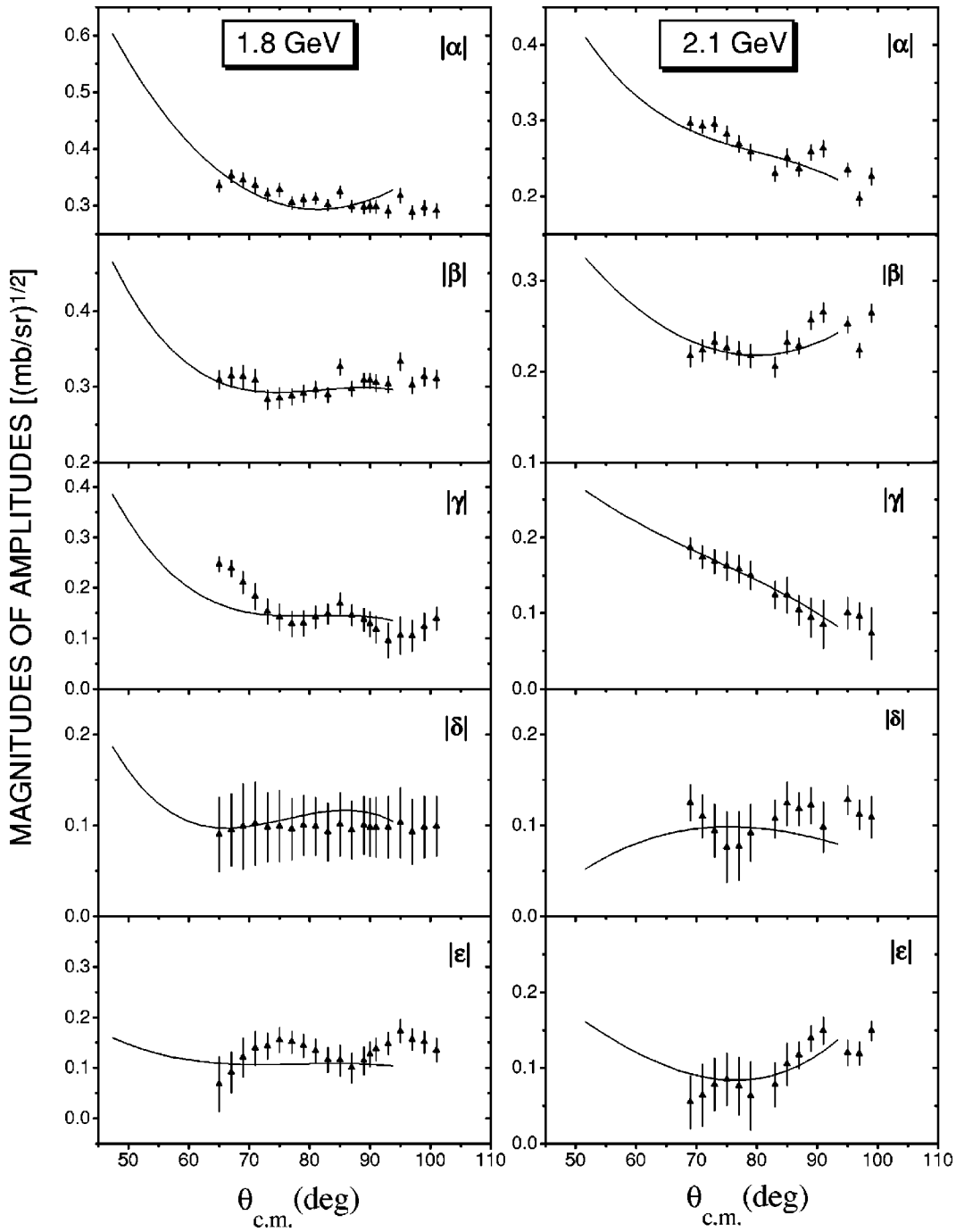

FIG. 1. The direct reconstruction of magnitudes of transversity amplitudes at 1.8 and 2.1 GeV. Triangles denote the present results and the solid lines correspond to the fitted amplitudes of Ref. [23].

The initial and final density matrices for the composite reaction is also defined in terms of the outer products of the constituent initial and final density matrices. Substituting all these into Eq. (12) generates the complete matrix elements of the p-p reaction matrix.

III. AMPLITUDE DETERMINATION AND SYMMETRY CONSTRAINTS

The optimal reaction matrix obtained contains 16 amplitudes and 256 bilinear combinations of amplitudes. In addition to Lorentz invariance upon imposition of all symmetry constraints such as parity, time reversal, and identical particles only five independent amplitudes survive, three of which are nonflip, and two of which are spin flip in the transversity frame. Depending upon the choice of frame (transversity or helicity or hybrid) the numbers of single-flip and double-flip are different. First, for simplicity, amplitude analysis is carried out in the transversity frame in which the direction of spin of each particle is normal to the reaction plane. We denote the invariant amplitudes as follows:

TABLE IV. Results of the real and imaginary parts of p-p scattering transversity amplitudes at 1.8 GeV.

$\theta_{\text{c.m.}}$	Re α	Re β	Re γ	Re δ	Re ε
65	0.193±0.028	0.196±0.023	−0.176±0.096	0.090±0.041	−0.039±0.050
67	0.245±0.022	0.191±0.025	−0.228±0.018	0.095±0.040	0.046±0.034
69	0.223±0.025	0.224±0.020	−0.175±0.025	0.099±0.047	0.093±0.035
71	0.203±0.027	0.254±0.017	−0.137±0.028	0.102±0.046	0.120±0.034
73	0.222±0.021	0.178±0.022	−0.142±0.024	0.098±0.038	0.109±0.022
75	0.261±0.016	0.212±0.018	−0.135±0.026	0.099±0.039	0.110±0.025
77	0.237±0.016	0.223±0.015	−0.128±0.025	0.096±0.034	0.097±0.020
79	0.248±0.015	0.209±0.018	−0.130±0.026	0.100±0.033	0.093±0.017
81	0.235±0.017	0.231±0.015	−0.142±0.023	0.099±0.032	0.086±0.018
83	0.217±0.018	0.222±0.015	−0.146±0.020	0.093±0.032	0.074±0.017
85	0.258±0.016	0.245±0.018	−0.167±0.020	0.101±0.035	0.074±0.020
87	0.226±0.016	0.225±0.016	−0.143±0.020	0.095±0.032	0.064±0.020
89	0.218±0.017	0.236±0.016	−0.136±0.023	0.100±0.032	0.073±0.018
90	0.227±0.016	0.236±0.016	−0.129±0.025	0.098±0.032	0.082±0.016
91	0.199±0.020	0.247±0.015	−0.117±0.027	0.098±0.033	0.088±0.017
93	0.166±0.024	0.242±0.015	−0.087±0.033	0.098±0.034	0.095±0.033
95	0.253±0.016	0.240±0.020	−0.103±0.036	0.103±0.039	0.111±0.022
97	0.231±0.015	0.209±0.020	−0.104±0.032	0.093±0.036	0.110±0.015
99	0.244±0.015	0.230±0.019	−0.123±0.028	0.098±0.034	0.097±0.014
101	0.247±0.014	0.232±0.018	−0.139±0.024	0.099±0.033	0.078±0.015

$\theta_{\text{c.m.}}$	Im α	Im β	Im γ	Im ε
65	0.274±0.019	0.239±0.019	0.173±0.061	−0.055±0.046
67	0.253±0.020	0.250±0.019	−0.069±0.062	−0.079±0.043
69	0.262±0.021	0.219±0.020	−0.119±0.035	−0.078±0.040
71	0.268±0.021	0.174±0.017	−0.121±0.033	−0.069±0.048
73	0.231±0.019	0.220±0.018	−0.055±0.017	−0.092±0.020
75	0.197±0.018	0.191±0.018	−0.042±0.012	−0.110±0.027
77	0.193±0.017	0.179±0.016	−0.016±0.017	−0.115±0.021
79	0.186±0.017	0.202±0.017	−0.005±0.027	−0.110±0.019
81	0.206±0.018	0.186±0.017	0.004±0.027	−0.103±0.020
83	0.209±0.017	0.184±0.016	0.023±0.039	−0.089±0.020
85	0.195±0.017	0.216±0.018	0.028±0.057	−0.088±0.024
87	0.195±0.017	0.194±0.017	0.030±0.055	−0.077±0.023
89	0.201±0.017	0.198±0.017	0.013±0.044	−0.087±0.022
90	0.194±0.017	0.198±0.017	0.009±0.046	−0.098±0.019
91	0.221±0.018	0.178±0.016	0.016±0.039	−0.105±0.020
93	0.238±0.018	0.182±0.016	0.039±0.043	−0.114±0.038
95	0.192±0.018	0.231±0.019	0.027±0.053	−0.133±0.024
97	0.172±0.016	0.218±0.018	0.013±0.052	−0.110±0.015
99	0.168±0.016	0.211±0.018	0.002±0.042	−0.116±0.017
101	0.154±0.015	0.206±0.018	−0.002±0.031	−0.111±0.020

$$D(++,++)=\alpha, \quad D(--,--)=\beta,$$

$$D(++,--)=\gamma, \tag{13}$$

$$D(+-,+-)=\delta, \quad D(+-,-+)=\varepsilon.$$

Of course, other groups use different notation such as $T1$-$T5$ for these amplitudes [14]. The relationship between these amplitudes and the measured experimental observables are given as [10]

$$\sigma P=|\alpha|^2-|\beta|^2, \tag{14}$$

$$\sigma=|\alpha|^2+|\beta|^2+2[|\gamma|^2+|\delta|^2+|\varepsilon|^2], \tag{15}$$

TABLE V. Results of the real and imaginary parts of p-p scattering transversity amplitudes at 2.1 GeV.

$\theta_{\text{c.m.}}$	Re α	Re β	Re γ	Re δ	Re ε
69	0.279±0.009	−0.214±0.023	0.004±0.005	0.125±0.020	−0.054±0.045
71	0.272±0.009	−0.139±0.043	0.055±0.009	0.110±0.024	−0.063±0.040
73	0.195±0.019	0.019±0.034	0.039±0.011	0.094±0.029	−0.078±0.035
75	0.198±0.017	0.100±0.023	0.030±0.029	0.076±0.039	−0.082±0.034
77	0.194±0.016	0.112±0.020	0.077±0.054	0.077±0.038	−0.075±0.038
79	0.167±0.018	0.091±0.023	0.147±0.046	0.092±0.031	−0.062±0.044
83	0.125±0.019	0.076±0.023	0.123±0.035	0.107±0.021	−0.076±0.028
85	0.108±0.027	0.115±0.021	0.117±0.035	0.124±0.024	−0.104±0.027
87	0.116±0.021	0.100±0.023	0.095±0.028	0.118±0.018	−0.117±0.018
89	0.129±0.023	0.114±0.025	0.093±0.032	0.122±0.020	−0.138±0.017
91	0.179±0.017	0.128±0.024	0.082±0.047	0.098±0.028	−0.149±0.019
95	0.071±0.028	0.146±0.020	0.099±0.026	0.128±0.016	−0.118±0.017
97	0.053±0.024	0.153±0.041	0.096±0.018	0.112±0.016	−0.091±0.013
99	0.059±0.028	0.203±0.014	0.068±0.031	0.109±0.023	−0.096±0.012

$\theta_{\text{c.m.}}$	Im α	Im β	Im γ	Im ε
69	−0.099±0.010	−0.035±0.062	0.186±0.014	0.010±0.012
71	−0.106±0.011	−0.174±0.028	0.165±0.015	0.011±0.013
73	−0.221±0.019	−0.232±0.013	0.164±0.016	−0.007±0.009
75	−0.200±0.018	−0.203±0.017	0.159±0.018	−0.022±0.010
77	−0.186±0.017	−0.189±0.017	0.139±0.024	−0.013±0.007
79	−0.197±0.017	−0.198±0.017	0.032±0.075	0.011±0.023
83	−0.193±0.016	−0.191±0.015	0.005±0.076	0.020±0.008
85	−0.227±0.018	−0.201±0.017	0.040±0.046	0.018±0.007
87	−0.206±0.015	−0.204±0.015	0.043±0.032	0.010±0.003
89	−0.223±0.017	−0.229±0.016	0.011±0.048	0.012±0.015
91	−0.192±0.017	−0.232±0.017	0.023±0.049	−0.013±0.019
95	−0.224±0.014	−0.205±0.017	0.015±0.042	0.021±0.008
97	−0.190±0.012	−0.163±0.081	0.004±0.017	0.077±0.013
99	−0.218±0.014	−0.169±0.016	−0.028±0.056	0.114±0.013

$$\sigma C_{NN}=|\alpha|^2+|\beta|^2+2[-|\gamma|^2+|\delta|^2-|\varepsilon|^2], \tag{16}$$

$$\sigma D_{NN}=|\alpha|^2+|\beta|^2+2[|\gamma|^2-|\delta|^2-|\varepsilon|^2], \tag{17}$$

$$\sigma K_{NN}=|\alpha|^2+|\beta|^2+2[-|\gamma|^2-|\delta|^2+|\varepsilon|^2], \tag{18}$$

$$\sigma C_{LL}=2\,\mathrm{Re}(\alpha+\beta)\delta^*+4\,\mathrm{Re}(\varepsilon^*\gamma), \tag{19}$$

$$\sigma C_{SS}=-2\,\mathrm{Re}(\alpha+\beta)\delta^*+4\,\mathrm{Re}(\varepsilon^*\gamma), \tag{20}$$

$$\sigma C_{LS}=2\,\mathrm{Im}(\alpha-\beta)\delta^*, \tag{21}$$

$$\sigma K_{SS}=-2\,\mathrm{Re}(\alpha+\beta)\varepsilon^*+4\,\mathrm{Re}(\gamma\delta^*), \tag{22}$$

$$\sigma H_{SNS}=-2\,\mathrm{Re}(\alpha-\beta)\varepsilon^*. \tag{23}$$

The five magnitudes are determined uniquely in terms of five observables as follows:

$$|\alpha|=\frac{\sqrt{\sigma}}{2\sqrt{2}}(1+C_{NN}+D_{NN}+K_{NN}+4P)^{1/2}, \tag{24}$$

$$|\beta|=\frac{\sqrt{\sigma}}{2\sqrt{2}}(1+C_{NN}+D_{NN}+K_{NN}-4P)^{1/2}, \tag{25}$$

$$|\gamma|=\frac{\sqrt{\sigma}}{2\sqrt{2}}(1-C_{NN}+D_{NN}-K_{NN})^{1/2}, \tag{26}$$

$$|\delta|=\frac{\sqrt{\sigma}}{2\sqrt{2}}(1+C_{NN}-D_{NN}-K_{NN})^{1/2}, \tag{27}$$

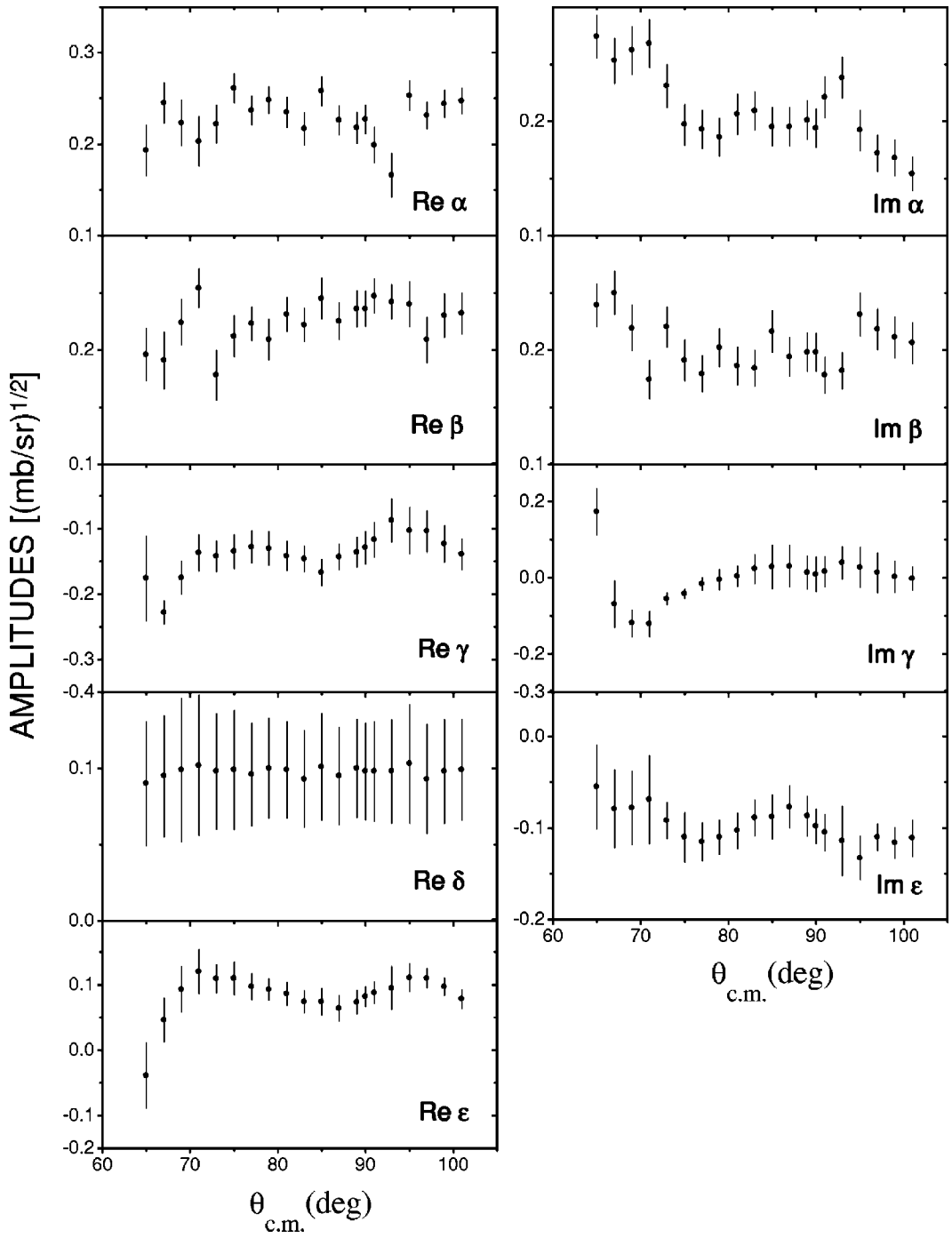

FIG. 2. The direct reconstruction of p-p elastic-scattering transversity amplitudes at 1.8 GeV. The real and imaginary parts of amplitudes α to ε are shown in $(\mathrm{mb/sr})^{1/2}$ as a function of the c.m. angle.

$$|\varepsilon| = \frac{\sqrt{\sigma}}{2\sqrt{2}}(1 - C_{NN} - D_{NN} + K_{NN})^{1/2}, \tag{28}$$

where C_{NN}, D_{NN}, K_{NN}, and P are polarization parameters measured experimentally over a long period of time at SATURNE II for energies 1.8 and 2.1 GeV and center-of-mass angle between 60° to 100°, and σ, the differential cross-section data are taken from EDDA [15]. For phase determination, since the overall phase is arbitrary, one of them, namely $\phi(\delta)$, is set equal to zero. Then, using the remaining equations (19)–(21), the following relations are obtained for $\phi(\alpha)$ and $\phi(\beta)$:

$$\sin\phi(\alpha) = \frac{\sigma C_{LS}}{2|\alpha||\delta|} + \frac{|\beta|}{|\alpha|}\sin\phi(\beta), \tag{29}$$

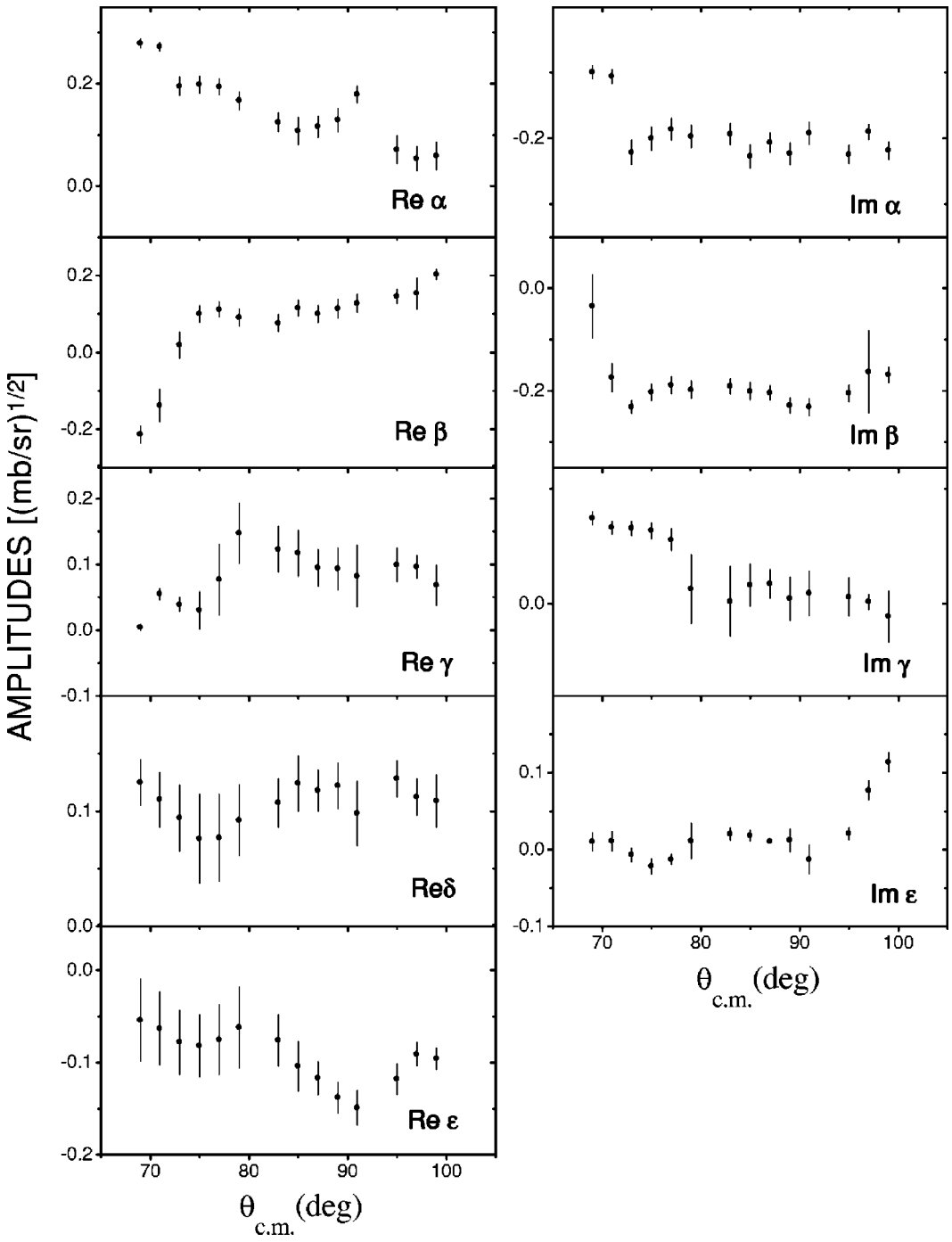

FIG. 3. The direct reconstruction of p-p elastic-scattering transversity amplitudes at 2.1 GeV. The real and imaginary parts of amplitudes α to ε are shown in $(\mathrm{mb/sr})^{1/2}$ as a function of the c.m. angle.

$$\cos\phi(\alpha)=\frac{\sigma C_{LL}-\sigma C_{SS}}{4|\alpha||\delta|}+\frac{|\beta|}{|\alpha|}\cos\phi(\beta). \tag{30}$$

These nonlinear equations have two solutions each for $\phi(\alpha)$ and $\phi(\beta)$. Particularly for some angles there exist no solutions and therefore were discarded. $\phi(\alpha)$ and $\phi(\beta)$ are given in terms of C_{LL}, C_{LS}, and C_{SS}. In a similar fashion the two remaining phases $\phi(\gamma)$ and $\phi(\varepsilon)$ are determined from equations relating them to the laboratory observables K_{SS} and H_{SNS}, which in turn are related to the center-of-mass observables and laboratory recoil angle [see Eq. (7.8) of Ref. [10]]. By eliminating $\phi(\gamma)$ between the two equations we obtain a relationship between $\phi(\varepsilon)$ and the difference $\phi(\gamma)-\phi(\varepsilon)$ in which all the other quantities are fixed. The difference $\phi(\gamma)-\phi(\varepsilon)$ is given in terms of C_{LL} and C_{SS}, which yield two different solutions. Therefore, altogether there are four different sets of phase parameters determining $\phi(\varepsilon)$. The best value of $\phi(\varepsilon)$ is taken to be the one with minimum χ^2.

TABLE VI. Results of p-p scattering helicity amplitudes at 1.8 GeV.

$\theta_{\text{c.m.}}$	Re a	Re b	Re c	Re d	Re e
65	-0.016 ± 0.029	-0.009 ± 0.016	0.035 ± 0.018	0.121 ± 0.037	-0.250 ± 0.492
67	-0.075 ± 0.169	-0.001 ± 0.003	0.065 ± 0.020	0.198 ± 0.020	-0.248 ± 0.482
69	-0.071 ± 0.158	-0.011 ± 0.021	0.120 ± 0.016	0.196 ± 0.017	-0.202 ± 0.393
71	-0.065 ± 0.147	-0.023 ± 0.044	0.157 ± 0.017	0.192 ± 0.017	-0.174 ± 0.335
73	-0.075 ± 0.163	-0.003 ± 0.010	0.133 ± 0.013	0.177 ± 0.013	-0.166 ± 0.323
75	-0.054 ± 0.122	-0.002 ± 0.005	0.155 ± 0.013	0.191 ± 0.013	-0.180 ± 0.353
77	-0.045 ± 0.105	-0.003 ± 0.008	0.147 ± 0.012	0.180 ± 0.012	-0.179 ± 0.350
79	-0.047 ± 0.109	0.004 ± 0.003	0.145 ± 0.012	0.175 ± 0.012	-0.183 ± 0.357
81	-0.047 ± 0.108	-0.005 ± 0.011	0.138 ± 0.012	0.181 ± 0.012	-0.194 ± 0.380
83	-0.047 ± 0.108	-0.006 ± 0.012	0.121 ± 0.013	0.173 ± 0.012	-0.192 ± 0.376
85	-0.045 ± 0.107	0.005 ± 0.006	0.130 ± 0.017	0.196 ± 0.014	-0.223 ± 0.436
87	-0.038 ± 0.094	0.005 ± 0.121	0.017 ± 0.169	0.014 ± 0.199	0.388 ± 0.151
89	-0.041 ± 0.100	-0.001 ± 0.002	0.132 ± 0.014	0.168 ± 0.013	-0.195 ± 0.381
90	-0.039 ± 0.095	0.001 ± 0.002	0.141 ± 0.014	0.172 ± 0.013	-0.188 ± 0.367
91	-0.040 ± 0.097	-0.011 ± 0.019	0.146 ± 0.014	0.165 ± 0.013	-0.175 ± 0.341
93	-0.038 ± 0.100	-0.014 ± 0.025	0.155 ± 0.016	0.144 ± 0.015	-0.147 ± 0.283
95	-0.035 ± 0.097	0.010 ± 0.007	0.179 ± 0.017	0.179 ± 0.016	-0.170 ± 0.328
97	-0.044 ± 0.108	0.012 ± 0.006	0.159 ± 0.015	0.171 ± 0.015	-0.154 ± 0.296
99	-0.041 ± 0.100	0.011 ± 0.006	0.155 ± 0.014	0.180 ± 0.013	-0.181 ± 0.352
101	-0.038 ± 0.092	0.013 ± 0.006	0.138 ± 0.012	0.178 ± 0.012	-0.200 ± 0.392
$\theta_{\text{c.m.}}$	Im a	Im b	Im c	Im d	Im e
65	0.242 ± 0.028	-0.001 ± 0.007	0.187 ± 0.028	0.014 ± 0.026	-0.069 ± 0.085
67	0.131 ± 0.125	0.014 ± 0.028	0.052 ± 0.018	0.121 ± 0.021	-0.199 ± 0.211
69	0.100 ± 0.095	0.000 ± 0.007	0.022 ± 0.017	0.141 ± 0.016	-0.218 ± 0.223
71	0.084 ± 0.075	-0.013 ± 0.030	0.015 ± 0.018	0.136 ± 0.017	-0.206 ± 0.212
73	0.131 ± 0.125	0.011 ± 0.021	0.039 ± 0.011	0.094 ± 0.011	-0.186 ± 0.191
75	0.131 ± 0.126	0.012 ± 0.025	0.021 ± 0.011	0.063 ± 0.011	-0.173 ± 0.178
77	0.143 ± 0.142	0.003 ± 0.004	0.028 ± 0.011	0.043 ± 0.011	-0.158 ± 0.162
79	0.150 ± 0.143	0.010 ± 0.005	0.040 ± 0.013	0.044 ± 0.013	-0.155 ± 0.159
81	0.151 ± 0.230	0.001 ± 0.003	0.049 ± 0.012	0.045 ± 0.013	-0.147 ± 0.151
83	0.154 ± 0.152	-0.001 ± 0.006	0.066 ± 0.014	0.042 ± 0.016	-0.131 ± 0.138
85	0.161 ± 0.154	0.003 ± 0.004	0.073 ± 0.018	0.045 ± 0.021	-0.133 ± 0.141
87	0.151 ± 0.145	0.000 ± 0.003	0.074 ± 0.017	0.044 ± 0.020	-0.121 ± 0.126
89	0.150 ± 0.146	-0.004 ± 0.011	0.063 ± 0.016	0.050 ± 0.017	-0.137 ± 0.143
90	0.151 ± 0.147	-0.002 ± 0.007	0.054 ± 0.016	0.045 ± 0.017	-0.142 ± 0.148
91	0.160 ± 0.158	-0.012 ± 0.026	0.056 ± 0.015	0.039 ± 0.016	-0.144 ± 0.149
93	0.182 ± 0.179	-0.019 ± 0.040	0.068 ± 0.017	0.029 ± 0.018	-0.142 ± 0.146
95	0.186 ± 0.182	0.003 ± 0.005	0.053 ± 0.019	0.026 ± 0.020	-0.159 ± 0.168
97	0.159 ± 0.156	0.005 ± 0.004	0.049 ± 0.018	0.036 ± 0.019	-0.146 ± 0.151
99	0.154 ± 0.151	0.004 ± 0.004	0.038 ± 0.016	0.036 ± 0.016	-0.152 ± 0.156
101	0.145 ± 0.144	0.004 ± 0.005	0.034 ± 0.013	0.036 ± 0.014	-0.146 ± 0.151

The observables used in the present analysis and their corresponding different notations of Argonne [25], Bystricky [14], Arndt [3], and the number of data points, references, and their χ^2 per number of data points are summarized in Table I. The magnitudes of transversity amplitudes are calculated and the results are given in Tables II and III and are shown in Fig. 1 for both energies. As shown in Fig. 1, our calculated amplitudes are compared with amplitudes reconstruction published recently [23]. Real and imaginary parts of the transversity amplitudes for both energies and the best solution are given in Tables IV and V, however, the latter are plotted in Figs. 2 and 3 for different c.m. angles at both

TABLE VII. Results of p-p scattering helicity amplitudes at 2.1 GeV.

$\theta_{\text{c.m.}}$	Re a	Re b	Re c	Re d	Re e
69	-0.017 ± 0.043	0.016 ± 0.001	0.054 ± 0.015	-0.075 ± 0.139	-0.104 ± 0.222
71	0.037 ± 0.018	-0.017 ± 0.026	0.084 ± 0.018	-0.081 ± 0.149	-0.092 ± 0.200
73	0.065 ± 0.014	-0.003 ± 0.006	0.081 ± 0.014	-0.052 ± 0.093	-0.120 ± 0.254
75	0.092 ± 0.017	-0.000 ± 0.002	0.087 ± 0.016	-0.020 ± 0.030	-0.138 ± 0.289
77	0.114 ± 0.024	-0.001 ± 0.002	0.116 ± 0.023	-0.038 ± 0.062	-0.114 ± 0.248
79	0.122 ± 0.025	0.000 ± 0.003	0.153 ± 0.024	-0.086 ± 0.156	-0.068 ± 0.165
83	0.097 ± 0.024	0.001 ± 0.001	0.128 ± 0.022	-0.103 ± 0.191	-0.080 ± 0.181
85	0.104 ± 0.018	0.006 ± 0.006	0.125 ± 0.018	-0.116 ± 0.221	-0.111 ± 0.237
87	0.101 ± 0.013	0.000 ± 0.001	0.102 ± 0.013	-0.111 ± 0.212	-0.124 ± 0.258
89	0.115 ± 0.017	-0.002 ± 0.004	0.099 ± 0.017	-0.116 ± 0.221	-0.144 ± 0.300
91	0.143 ± 0.019	-0.010 ± 0.025	0.092 ± 0.020	-0.087 ± 0.161	-0.159 ± 0.329
95	0.098 ± 0.016	0.005 ± 0.004	0.109 ± 0.015	-0.118 ± 0.227	-0.128 ± 0.266
97	0.089 ± 0.035	0.007 ± 0.013	0.110 ± 0.025	-0.099 ± 0.180	-0.105 ± 0.238
99	0.093 ± 0.019	0.012 ± 0.004	0.106 ± 0.016	-0.071 ± 0.134	-0.134 ± 0.282
$\theta_{\text{c.m.}}$	Im a	Im b	Im c	Im d	Im e
69	0.055 ± 0.045	0.123 ± 0.006	0.064 ± 0.015	-0.122 ± 0.251	0.131 ± 0.250
71	0.007 ± 0.010	0.103 ± 0.105	0.018 ± 0.010	-0.147 ± 0.300	0.158 ± 0.305
73	-0.028 ± 0.012	0.044 ± 0.088	-0.035 ± 0.012	-0.198 ± 0.400	0.192 ± 0.374
75	-0.010 ± 0.010	0.025 ± 0.050	-0.032 ± 0.012	-0.191 ± 0.383	0.169 ± 0.328
77	-0.018 ± 0.012	0.020 ± 0.041	-0.031 ± 0.014	-0.170 ± 0.342	0.157 ± 0.298
79	-0.088 ± 0.030	0.019 ± 0.039	-0.077 ± 0.029	-0.109 ± 0.231	0.120 ± 0.221
83	-0.104 ± 0.026	0.012 ± 0.007	-0.083 ± 0.027	-0.088 ± 0.192	0.109 ± 0.200
85	-0.096 ± 0.020	-0.002 ± 0.007	-0.078 ± 0.019	-0.118 ± 0.246	0.136 ± 0.258
87	-0.086 ± 0.014	0.004 ± 0.008	-0.076 ± 0.014	-0.119 ± 0.246	0.129 ± 0.248
89	-0.114 ± 0.019	0.004 ± 0.008	-0.102 ± 0.019	-0.112 ± 0.236	0.125 ± 0.235
91	-0.088 ± 0.021	0.013 ± 0.021	-0.101 ± 0.022	-0.124 ± 0.257	0.111 ± 0.205
95	-0.110 ± 0.016	-0.019 ± 0.008	-0.090 ± 0.016	-0.104 ± 0.219	0.125 ± 0.238
97	-0.124 ± 0.039	-0.025 ± 0.047	-0.048 ± 0.043	-0.052 ± 0.130	0.129 ± 0.231
99	-0.168 ± 0.020	-0.036 ± 0.007	-0.053 ± 0.021	-0.025 ± 0.067	0.140 ± 0.266

energies. Fortunately the χ^2 for each set of solutions were distinct enough to allow an easy selection of the minimum. In a way this may be an indication of the self-consistency of the extra and interpolated data set used here. As a check, our amplitudes do satisfy the following symmetry relations which are the results of imposing the Pauli principle in the transversity frame [14]:

$$\alpha(\theta)=\beta(\pi-\theta), \tag{31}$$

$$\gamma(\theta)=\varepsilon(\pi-\theta), \tag{32}$$

$$\delta(\theta)=\delta(\pi-\theta). \tag{33}$$

Once the transversity amplitudes have been determined, the helicity amplitudes are easily obtained by the mathematical method described in Ref. [10] and are denoted by a, b, c, d, and e. Due to the existence of the relationship between helicity and transversity amplitudes, four sets of solutions in the helicity frame seem to be inevitable. The real and imaginary parts of the best helicity amplitudes have been given in Tables VI and VII and also plotted in Figs. 4 and 5 for different c.m. angles at both energies.

IV. CONCLUSION

This nondynamical amplitude analysis in optimal formalism at 1.8 and 2.1 GeV allows an accurate determination of the complex amplitudes in transversity as well as helicity frame, provided that a complete set of observables is measured. It is suggested that C_{LL} and C_{SS} be updated by experimentalists for more reliable conclusions. In the transversity frame, the magnitudes of the five amplitudes were obtained without any ambiguity. These magnitudes exhibit almost the same variations as a function of c.m. angle at both energies. Phase calculations are confronted with four distinct solutions, one of which is selected based on minimum χ^2

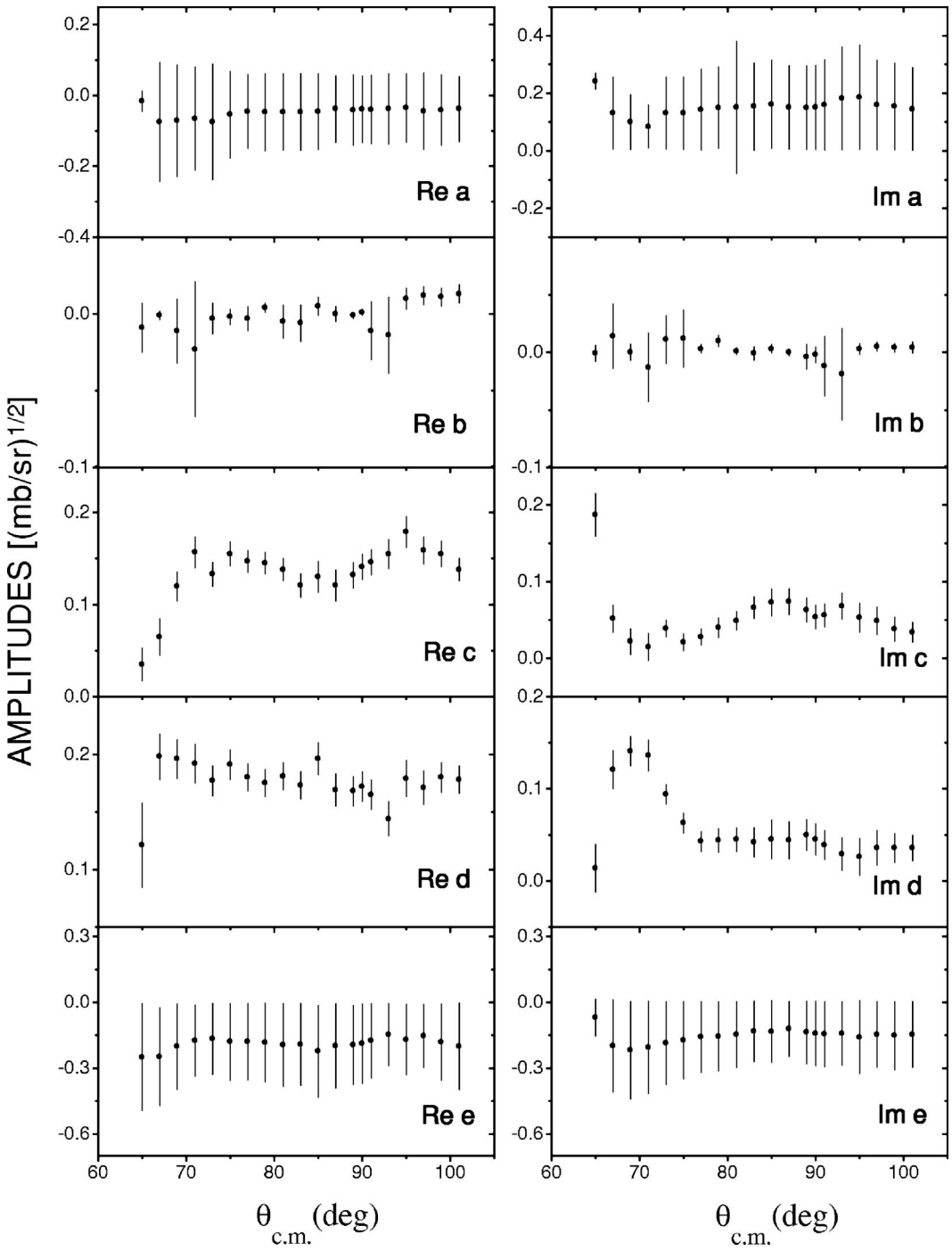

FIG. 4. The direct reconstruction of p-p elastic scattering helicity amplitudes at 1.8 GeV. The real and imaginary parts of amplitudes a to e are shown in $(\mathrm{mb/sr})^{1/2}$ as a function of the c.m. angle.

criteria. Our interpolated data exhibit several imaginary solutions in the range of 60° to 68° c.m. angle at 2.1 GeV which were disregarded. Such unexpected solutions may be caused by excess uncertainties in experimental data. The error bars were obtained by the standard error propagation method and are indicated at each point. As shown at some point, error bars are relatively large due to the existence of large errors in the corresponding observables. In the helicity frame, the magnitudes have no ambiguity, but in phase calculation there exist several angles in which some phases possess large uncertainties attributed to data points. At both energies the magnitudes of two nonflip $|\alpha|$ and $|\gamma|$ decrease quite slowly as the c.m. angles increase. The remaining amplitudes vary in different ways. For example, while the nonflip $|\beta|$ and double flip $|\delta|$ are almost independent of c.m. angle θ, double flip $|\varepsilon|$ exhibit some fluctuations in the same angular region. In the helicity frame the real and imaginary parts of all amplitudes for angles larger than 70° are almost independent of c.m. angle θ. As is shown in Tables II and III, the symmetry relations between the magnitudes of am-

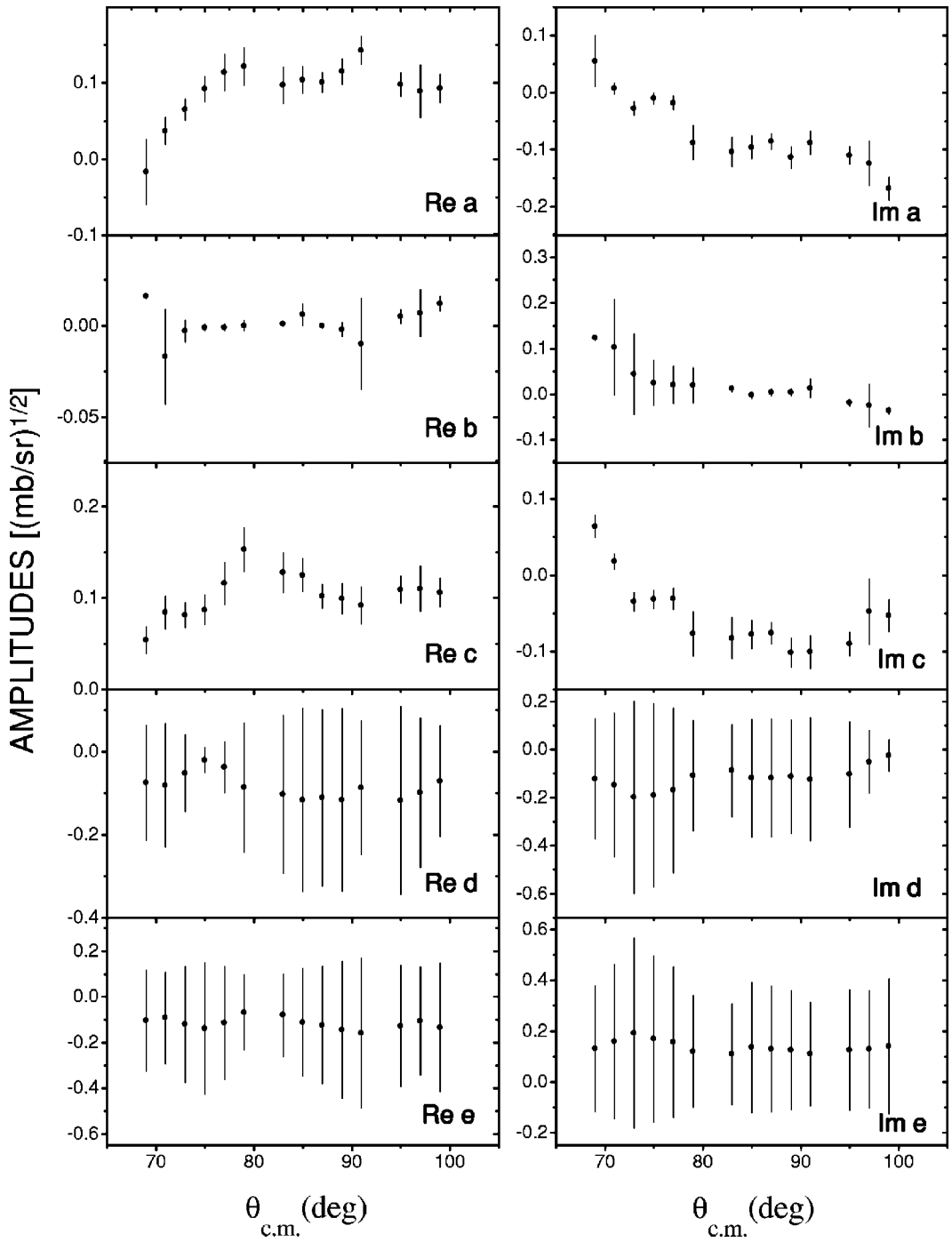

FIG. 5. The direct reconstruction of p-p elastic scattering helicity amplitudes at 2.1 GeV. The real and imaginary parts of amplitudes a to e are shown in $(\mathrm{mb/sr})^{1/2}$ as a function of the c.m. angle.

plitudes around θ and $\pi-\theta$ hold. Comparison of our constructed amplitudes with those obtained in Ref. [23] indicate that our results within corresponding errors are in a good agreement with those obtained by them. Considering the fact that our results are obtained by using only ten observables, required by a complete set, one may conclude that this is more economical.

ACKNOWLEDGMENTS

The partial support of the Shiraz University Research Council is appreciated. The authors appreciate the cooperation of Professor F. Lehar, Professor H. Spinka, Professor G. Goldstein, and Dr. C. Allgower in this work.

[1] A. Martin, R. Birsa, K. Bos, F. Bradamente, D. V. Bugg, S. Daila Torre-Colautti, J. R. Hall, E. Heer, R. Hess, J. C. Kluyver, R. A. Kunne, C. Lechanoine-LeLuc, A. Penzo, D. Rapin, P. Shitavon, F. Tessarotto, A. Villari, and A. M. Zanetti, Nucl. Phys. **A487**, 563 (1988).

[2] R. A. Arndt, L. D. Roper, R. A. Bryan, R. B. Clark, B. J. VerWest, and P. Signell, Phys. Rev. D **28**, 97 (1983).

[3] R. A. Arndt, L. D. Roper, R. L. Workman, and M. W. McNaughton, Phys. Rev. D **45**, 3995 (1992); R. A. Arndt, I. I. Strakovsky, and R. L. Workman, Phys. Rev. C **50**, 2731 (1994); R. A. Arndt, C. H. Oh, I. I. Strakovsky, R. L. Workman, and F. Dohrman, *ibid.* **56**, 3005 (1997).

[4] G. R. Goldstein and M. J. Moravcsik, Ann. Phys. (N.Y.) **98**, 128 (1976).

[5] N. Ghahramany, G. R. Goldstein, and M. J. Moravcsik, Phys. Rev. D **28**, 1086 (1983).

[6] M. J. Moravcsik, N. Ghahramany, and G. R. Goldstein, Phys. Rev. D **30**, 1899 (1984).

[7] J. Ball *et al.*, Nuovo Cimento A **111**, 13 (1998); G. R. Goldstein, M. J. Moravcsik, and D. Bregman, Lett. Nuovo Cimento **11**, 137 (1974).

[8] J. Bystricky, F. Lehar, J. Patera, and P. Winternitz, Lect. Notes Phys. **87**, 509 (1978).

[9] C. Lechanoine-Leluc and F. Lehar, Rev. Mod. Phys. **65**, 47 (1993).

[10] G. R. Goldstein and M. J. Moravcsik, Ann. Phys. (N.Y.) **142**, 219 (1982).

[11] R. Reid and M. J. Moravcsik, Ann. Phys. (N.Y.) **84**, 535 (1974), and references therein.

[12] M. J. Moravcsik, Phys. Rev. D **22**, 135 (1980).

[13] P. L. Csonka, M. J. Moravcsik, and M. D. Scadron, Ann. Phys. (N.Y.) **41**, 1 (1967).

[14] J. Bystricky, F. Lehar, and P. Winternitz, J. Phys. (Paris) **39**, 1 (1978).

[15] EDDA Collaboration, D. Albers, J. Bisplinghoff, R. Bollmann, K. Busser, P. Cloth, R. Daniel, O. Diehl, F. Dohrmann, H. P. Engelhardt, J. Ernst, P. D. Eversheim, M. Gasthuber, R. Gebel, A. Gross, R. Gross-Hardt, S. Heider, A. Heine, F. Hinterberger, M. Igelbrink, R. Jahn, M. Jeske, U. Lahr, R. Langkau, J. Lindlein, R. Maier, R. Maschuw, T. Mayer-Kuckuk, F. Mosel, M. Muller, M. Munstermann, D. Prasuhn, H. Rohdjess, D. Rosendaal, U. Ross, P. Von Rossen, H. Scheid, N. Schirm, M. Schulz-Rojahn, F. Schwandt, V. Schwarz, W. Scobel, G. Sterzenbach, H. J. Trelle, A. Wellinghausen, W. Wiedmann, K. Woller, and R. Ziegler, Phys. Rev. Lett. **78**, 1652 (1997).

[16] C. E. Allgower, J. Ball, L. S. Barabash, M. Beddo, Y. Bedfer, A. Boutefnouchet, J. Bystricky, Ph. Demierre, J. M. Fontaine, V. Ghazikhanian, D. Grosnick, R. Hess, Z. Janout, Z. F. Janout, V. A. Kalinnikov, T. E. Kasprzyk, Yu. M. Kazarinov, B. A. Khachaturov, R. Kunne, F. Lehar, A. de Lesquen, D. Lopiano, M. de Mali, V. N. Matafonov, I. L. Pisarev, A. A. Popov, A. N. Prokofiev, D. Rapin, J. L. Sans, H. M. Spinka, S. Trentalange, Yu. A. Usov, V. V. Vikhrov, B. Vuaridel, C. A. Whitten, and A. A. Zhdanov, Eur. Phys. J. C **1**, 131 (1998).

[17] F. Lehar, A. de Lesquen, J. P. Meyer, L. Van Rossum, P. Chaumette, J. Deregel, J. Fabre, J. M. Fontaine, F. Perrot, J. Ball, C. D. Lac, A. Michalowicz, Y. Onel, D. Adams, J. Bystricky, V. Ghazikhanian, C. A. Whitten, and A. Penzo, Nucl. Phys. **B294**, 1013 (1987).

[18] C. E. Allgower, Ph.D. thesis, Arizona State University, 1997.

[19] F. Lehar, A. de Lesquen, L. Van Rossum, J. M. Fontaine, F. Perrot, P. Chaumette, J. Deregel, J. Fabre, J. Ball, C. D. Lac, Y. Onel, A. Michalowicz, J. Bystricky, and V. Ghazikhanian, Nucl. Phys. **B296**, 535 (1988).

[20] SAID Program, Solution SM 99.

[21] C. E. Allgower, J. Ball, M. Beddo, Y. Bedfer, A. Boutefnouchet, J. Bystricky, P. A. Chamouard, Ph. Demierre, J. M. Fontaine, V. Ghazikhanian, D. Grosnick, R. Hess, Z. Janout, Z. F. Janout, V. A. Kalinnikov, T. E. Kasprzyk, B. A. Khachaturov, R. Kunne, F. Lehar, A. de Lesquen, D. Lopiano, V. N. Matafonov, I. L. Pisarev, A. A. Popov, A. N. Prokofiev, D. Rapin, J. L. Sans, H. M. Spinka, A. Teglia, Yu. A. Usov, V. V. Vikhrov, B. Vuaridel, C. A. Whitten, and A. A. Zhdanov, Nucl. Phys. **A637**, 231 (1998).

[22] C. E. Allgower, J. Ball, L. S. Barabash, M. Beddo, Y. Bedfer, A. Boutefnouchet, J. Bystricky, Ph. Demierre, J. M. Fontaine, V. Ghazikhanian, D. Grosnick, R. Hess, Z. Janout, Z. F. Janout, V. A. Kalinnikov, T. E. Kasprzyk, Yu. M. Kazarinov, B. A. Khachaturov, R. Kunne, C. Lechanoine-Leluc, F. Lehar, A. de Lesquen, D. Lopiano, M. de Mali, V. N. Matafonov, I. L. Pisarev, A. A. Popov, A. N. Prokofiev, D. Rapin, J. L. Sans, H. M. Spinka, Yu. A. Usov, V. V. Vikhrov, B. Vuaridel, C. A. Whitten, and A. A. Zhdanov, Eur. Phys. J. C **5**, 453 (1998).

[23] J. Bystricky, C. Lechanoine-LeLuc, and F. Lehar, Eur. Phys. J. C **4**, 607 (1998).

[24] F. Perrot, J. M. Fontaine, F. Lehar, A. de Lesquen, J. P. Meyer, L. Van Rossum, P. Chaumette, J. Deregel, J. Fabre, J. Ball, C. D. Lac, A. Michalowicz, Y. Onel, B. Aas, D. Adams, J. Bystricky, V. Ghazikhanian, G. Igo, F. Sperisen, C. A. Whitten, and A. Penzo, Nucl. Phys. **B294**, 1001 (1987).

[25] A. Beretvas, D. Miller, I. P. Auer, R. Giese, K. Nield, P. Rynes, B. Sandler, Y. Watanabe, and A. Yokosawa, Phys. Rev. D **20**, 21 (1979).